EBOLA VIRUS

Two-pore channels control Ebola virus host cell entry and are drug targets for disease treatment

Yasuteru Sakurai,[1] Andrey A. Kolokoltsov,[2] Cheng-Chang Chen,[3] Michael W. Tidwell,[4] William E. Bauta,[4] Norbert Klugbauer,[5] Christian Grimm,[3] Christian Wahl-Schott,[3] Martin Biel,[3] Robert A. Davey[1]*

Ebola virus causes sporadic outbreaks of lethal hemorrhagic fever in humans, but there is no currently approved therapy. Cells take up Ebola virus by macropinocytosis, followed by trafficking through endosomal vesicles. However, few factors controlling endosomal virus movement are known. Here we find that Ebola virus entry into host cells requires the endosomal calcium channels called two-pore channels (TPCs). Disrupting TPC function by gene knockout, small interfering RNAs, or small-molecule inhibitors halted virus trafficking and prevented infection. Tetrandrine, the most potent small molecule that we tested, inhibited infection of human macrophages, the primary target of Ebola virus in vivo, and also showed therapeutic efficacy in mice. Therefore, TPC proteins play a key role in Ebola virus infection and may be effective targets for antiviral therapy.

Ebola viruses (EBOVs), together with Marburgvirus, are a highly diverse group of viruses that constitute the *Filoviridae*. Almost all of them, including the strain responsible for the latest outbreak in West Africa, cause a highly lethal, rapidly progressing hemorrhagic fever in humans and nonhuman primates (*1*, *2*). However, there is currently no licensed drug treatment or broadly active vaccine (*3*), making them important public health threats and potential biothreat agents. Because, like most viruses, EBOV depends on host cell factors to complete its life cycle (*4*), blocking such interactions may have a large impact on infection and disease outcome. Recent successes in cell culture and some animal models suggest that this approach holds promise for rapidly bringing new drugs to the clinic (*5*).

EBOV binds to several types of cell surface proteins to initiate host cell entry (*6*–*8*), after which it is internalized by macropinocytosis and follows an endosomal route to reach acidic compartments (*9*, *10*). There, host proteases such as cathepsins cleave the viral glycoproteins (GPs) (*11*), which bind to the endosomal membrane protein, NPC1, and eventually facilitate the release of the viral core to the cell cytoplasm, where replication begins (*12*, *13*). Previously, we showed that host calcium signaling proteins were important for EBOV host cell entry but were unable to identify the functional mechanism nor address whether they could be therapeutic targets (*14*).

To identify and characterize upstream effectors regulating calcium signaling in the context of EBOV infection, we tested the importance of calcium channels using antagonists for each of the four common channel types (Fig. 1, A to C, and fig. S1). Only compounds blocking L-type channels inhibited EBOV infection in HeLa cells, which is consistent with previous reports (*15*, *16*). Verapamil, a drug approved by the U.S. Food and Drug Administration (FDA) to treat cardiovascular diseases, efficiently inhibited EBOV infection with a half-maximal inhibitory concentration (IC_{50}) of 4 μM (Fig. 1A). Similarly, two other structurally distinct L-type channel antagonists, nimodipine and diltiazem, also reduced EBOV infection efficiency (fig. S1, A and B). Tetrandrine, originally isolated from Chinese and Japanese herbs but now produced synthetically, was especially potent, with an IC_{50} of 55 nM (Fig. 1B). By contrast, gabapentin, representing a fifth distinct class of L-type channel inhibitor, had no effect, even at high concentrations (Fig. 1C). This finding suggested that classical L-type channels were not the upstream factor in EBOV calcium-channel dependence. Recently, verapamil, nimodipine, and diltiazem were shown to also

[1]Texas Biomedical Research Institute, San Antonio, TX, USA. [2]The University of Texas Medical Branch, Galveston, TX, USA. [3]Center for Integrated Protein Science Munich (CIPSM) at the Department of Pharmacy–Center for Drug Research, Ludwig-Maximilians-Universität München, Munich, Germany. [4]Southwest Research Institute, San Antonio, TX, USA. [5]Institute for Experimental and Clinical Pharmacology and Toxicology, Albert-Ludwigs-Universität Freiburg, Freiburg, Germany.
*Corresponding author. E-mail: rdavey@txbiomed.org

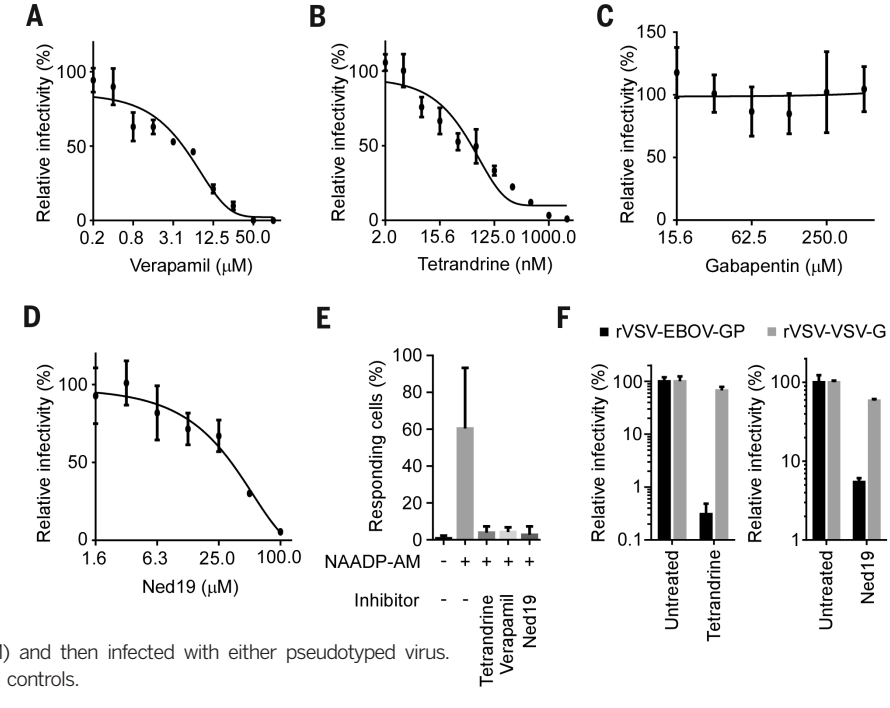

Fig. 1. Inhibitors of NAADP signaling block EBOV infection. Dose-response curves for verapamil (**A**), tetrandrine (**B**), gabapentin (**C**), and Ned19 (**D**) were determined by pretreating HeLa cells with the indicated doses of each compound and then infecting the cells with a recombinant EBOV encoding green fluorescent protein (GFP) as a marker of infection (EBOV-GFP). Infection efficiencies were calculated by dividing the numbers of GFP-positive cells by those of total cells and normalizing the infectivity to untreated cells (mean ± SD, n = 3). Each data set is representative of three independent experiments. (**E**) The effect of the indicated compounds on NAADP-stimulated calcium release was measured by stimulating cells with 1 μM NAADP-AM (*30*, *31*) or control dimethyl sulfoxide and imaging cell fluorescence after addition of the calcium-sensitive dye Fluo-4. Cells showing $F_{max}/F_0 > 2$ (F_{max}: maximum fluorescence intensity; F_0: mean fluorescence intensity before stimulation) were counted as responsive cells. At least 800 cells were analyzed for each treatment, and data averaged over three experiments ± SD. (**F**) Pseudotyped viruses bearing the glycoproteins of EBOV (rVSV-EBOV-GP) or VSV (rVSV-VSV-G) and encoding firefly luciferase as an infection marker were used to show entry dependence of EBOV on NAADP signaling. Cells were treated with tetrandrine (2 μM) or Ned19 (100 μM) and then infected with either pseudotyped virus. Luciferase activities were normalized to those of untreated controls.

inhibit calcium signaling triggered by nicotinic acid adenine dinucleotide phosphate (NAADP) (*17*). NAADP is a highly potent intracellular calcium–mobilizing agent and stimulates intracellular calcium channels to release Ca^{2+} from endosomes and lysosomes (*18*). This pathway is specifically blocked by the small-molecule antagonist Ned19 (*19*). We found that Ned19 also blocked EBOV infection (Fig. 1D). All inhibitors tested showed

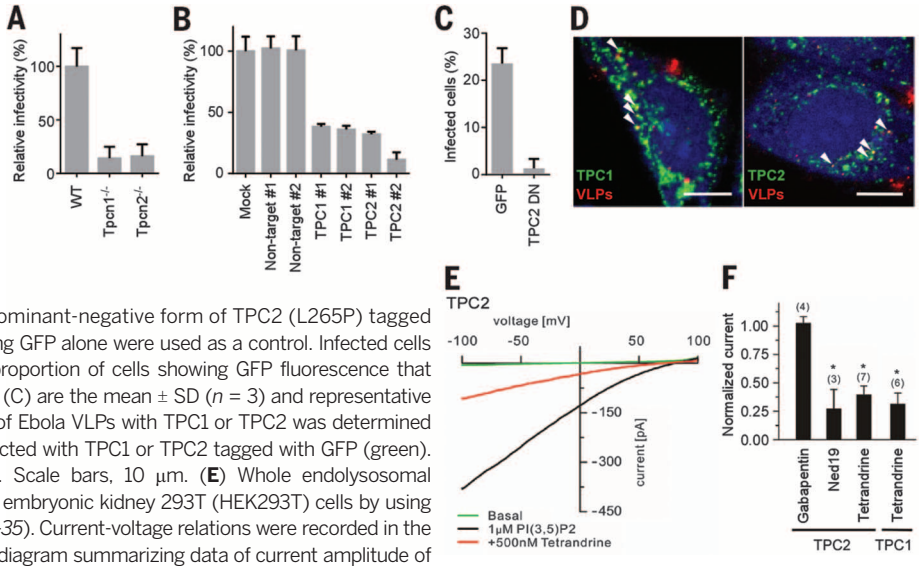

Fig. 2. The endosomal calcium channels TPC1 and TPC2 are necessary for EBOV infection. (**A**) MEFs from wild-type (WT), *Tpcn1*$^{-/-}$, or *Tpcn2*$^{-/-}$ mice (*25*, *32*) were infected with EBOV-GFP. The frequency of GFP-positive cells in the total cell population was normalized to that of total cells. (**B**) HeLa cells were transfected with either two independent nontargeting, TPC1-specific, or TPC2-specific siRNAs and infected with EBOV-GFP. The frequency of GFP-positive cells in the total cell population was normalized to that of mock-transfected cells. (**C**) HeLa cells overexpressing a dominant-negative form of TPC2 (L265P) tagged with GFP were infected with WT EBOV. Cells expressing GFP alone were used as a control. Infected cells were detected with antibody against EBOV GP. The proportion of cells showing GFP fluorescence that were infected was calculated. All data for (A), (B), and (C) are the mean ± SD (n = 3) and representative of three independent experiments. (**D**) Colocalization of Ebola VLPs with TPC1 or TPC2 was determined by incubating VLPs (red) for 2 hours with cells transfected with TPC1 or TPC2 tagged with GFP (green). Colocalized particles were indicated by arrowheads. Scale bars, 10 μm. (**E**) Whole endolysosomal currents were recorded from TPC2-expressing human embryonic kidney 293T (HEK293T) cells by using modified conventional patch-clamp with $PI(3,5)P_2$ (*33*–*35*). Current-voltage relations were recorded in the presence or absence of tetrandrine (500 nM). (**F**) Bar diagram summarizing data of current amplitude of TPC2 or TPC1 in the presence of gabapentin (100 μM), Ned19 (200 μM), or tetrandrine (500 nM), normalized to those before drug application. *P < 0.001 using analysis of variance, compared to current in the presence of gabapentin for TPC2 or without inhibitors for TPC1. Data are the mean ± SEM.

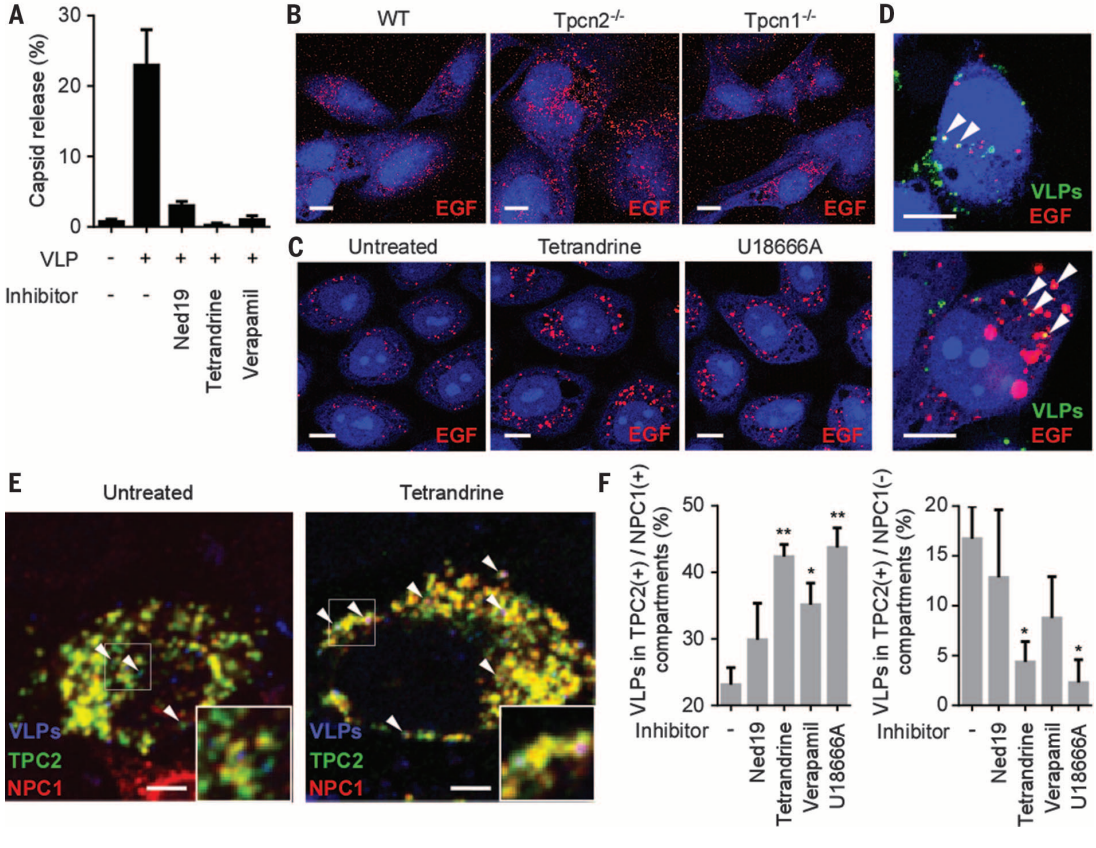

Fig. 3. Blocking TPC function affects EBOV entry through endosomal compartments. (**A**) VLPs loaded with β-lactamase were used to measure membrane fusion and virus capsid release into the cytoplasm after each treatment (as for fig. S10). The number of cells showing signal was divided by the number of total cells. (**B**) Evaluation of EGF trafficking in TPC knockout cells. Representative confocal images of WT, *Tpcn2*$^{-/-}$, and *Tpcn1*$^{-/-}$ MEFs incubated with AlexaFluor555-EGF. (**C**) Evaluation of EGF trafficking in tetrandrine or U18666A-treated cells. Representative confocal images of HeLa cells incubated with AlexaFluor555-EGF (red) in the presence or absence of tetrandrine or U18666A. (**D**) Colocalization of Ebola VLPs and EGF. HeLa cells were incubated with AlexaFluor555-EGF (red) for 30 min followed by Ebola VLPs (green) for 3.5 hours in the presence of tetrandrine. VLPs were stained with a GP-specific antibody. Examples of colocalized particles are indicated by arrowheads. Scale bars (B to D): 10 μm. (**E**) Effect of tetrandrine on colocalization of Ebola VLPs with TPC2- and/or NPC1-positive endosomes was measured. HeLa cells overexpressing GFP-tagged TPC2 (green) and Myc-tagged NPC1 (red) were pretreated with inhibitors and incubated with VLPs (blue) for 4 hours. Insets show magnified areas of the image, and arrowheads indicate examples of VLPs that are associated with the TPC2(+)/NPC1(−) compartment (left panel) or the TPC2(+)/NPC1(+) compartment (right panel). Scale bars, 5 μm. (**F**) In the presence of the indicated inhibitors, the ratio of VLPs colocalizing with the TPC2(+)/NPC1(+) compartment (left) or the TPC2 (+)/NPC1(−) compartment (right) was calculated. *P < 0.05 and **P < 0.005, using unpaired Student's t test to compare treated to untreated cells. Data are the mean ± SEM (n = 3 or 4).

no cytotoxicity at the highest concentration used (fig. S2). Like verapamil and Ned19, tetrandrine was also a potent inhibitor of NAADP-stimulated calcium release (Fig. 1E and fig. S3). These results suggested a role for NAADP-stimulated calcium channels in EBOV infection and that tetrandrine could block this host factor.

NAADP has been suggested to regulate endosome maturation through vesicular fusion and trafficking (*20*). This would suggest a role in virus entry into cells, which was tested with pseudotyped viruses. Infection of cells by recombinant vesicular stomatitis virus bearing the glycoprotein of EBOV (rVSV-EBOV-GP) was highly sensitive to tetrandrine, verapamil, or Ned19 (Fig. 1F and fig. S4A). This suggests that NAADP-stimulated channel activity specifically affects the GP-mediated entry step of EBOV. Moreover, tetrandrine and verapamil potently inhibited infection of recombinant VSV bearing Marburgvirus glycoprotein, but inhibited infection only weakly for VSV, Lassa virus, Venezuelan equine encephalitis virus, or Rabies virus (Fig. 1F and fig. S4, B and C), suggesting that filoviruses are much more dependent on this pathway than are other virus types.

To gain further insight into the connection between the NAADP-mediated pathway and EBOV infection, we sought to identify the effector calcium channel required for the infection. Recent studies have shown that two-pore channels (TPCs) are the major calcium channels activated by NAADP (*21*). They are also activated by the phosphatidylinositol 3,5-bisphosphate [$PI(3,5)P_2$] and are highly conserved proteins with both TPC1 and TPC2 present in humans, mice, and other animals (*22*). We found that mouse embryonic fibroblasts (MEFs) lacking TPC1 or TPC2 expression ($Tpcn1^{-/-}$ or $Tpcn2^{-/-}$) resisted EBOV infection (Fig. 2A). Overexpression of human TPCs in the mutant cells significantly recovered the infectivity (fig. S5), suggesting the specific effects of gene knockout. Similarly, even though suppression of TPC expression by small interfering RNAs (siRNAs) was incomplete (fig. S6), EBOV infection was reduced in HeLa cells transfected with either TPC1 or TPC2 siRNAs (Fig. 2B). In addition, overexpression of a dominant-negative form of TPC2, which was reported to efficiently block NAADP-stimulated calcium release (*23*), inhibited EBOV infection (Fig. 2C). Furthermore, Ebola virus-like particles (VLPs) incubated with cells localized to TPC1- and TPC2-positive endosomal compartments (Fig. 2D). Whole endolysosomal patch-clamp analyses showed that tetrandrine blocked both TPC1- and TPC2-mediated current elicited by $PI(3,5)P_2$ as well as NAADP (Fig. 2, E and F, and fig. S7). In contrast, gabapentin, which did not inhibit virus infection, had no effect on TPC2 function. Together, our data showed that TPCs, the effector channels of NAADP and $PI(3,5)P_2$-mediated signaling, are important for EBOV infection, probably while virus is inside endosomes. Calcium channel inhibitors targeted TPCs, with tetrandrine being the most potent.

During host cell entry, EBOV is transported to acidic endosomes, which express lysosomal-associated membrane protein 1 (LAMP1) (*9*). We found that VLPs still localized to LAMP1-positive vesicles in $Tpcn1^{-/-}$ and $Tpcn2^{-/-}$ MEFs, as well as inhibitor-treated cells (fig. S8), indicating that this step was unaffected. The EBOV GP is then cleaved by endosomal cysteine proteases before virus-endosome membrane fusion can occur (*11*), and so we next examined whether precleaved GPs could overcome the action of the inhibitory drugs using rVSV-EBOV-GP pretreated with the protease thermolysin. Treatment with Ned19, tetrandrine, or verapamil still efficiently blocked precleaved virus infection, but a control cysteine protease inhibitor, E-64-D, did not (fig. S9), indicating that the calcium channel inhibitors affect a late entry step after GP proteolysis in endosomes. When membrane fusion was evaluated, with a virus contents release assay (*24*), these inhibitors significantly reduced the contents mixing signal (Fig. 3A and fig. S10), indicating that virus-endosome membrane fusion and virus capsid release into the cell cytoplasm were arrested.

A recent study showed that blocking TPC2 function resulted in accumulation of epidermal growth factor (EGF) in LAMP1-positive endosomal compartments, suggesting a block of endosomal trafficking in these acidic compartments (*25*). We found that tetrandrine-treated HeLa cells showed a similar accumulation of EGF, as well as $Tpcn2^{-/-}$ MEFs, whereas $Tpcn1^{-/-}$ MEFs showed less EGF accumulation (Fig. 3, B and C). Moreover, Ebola VLPs and EGF colocalized in tetrandrine-treated cells (Fig. 3D), suggesting that both use or converge upon a common endosomal trafficking route that is regulated by TPCs. Previously, EBOV entry was shown to be dependent on another endosomal protein, NPC1 (*12*, *13*). The small molecule U18666A induces a phenotype that mimics NPC1 deficiency, leading to cholesterol accumulation in endosomes. When cells were treated with U18666A, the pattern of EGF accumulation was similar to that seen after treatment with tetrandrine (Fig. 3C). Moreover, treatment of rVSV-EBOV-GP–infected cells with verapamil or U18666A revealed similar inhibitory kinetics, with each becoming ineffective when the drug was added 1.5 to 2 hours after infection (fig. S11), suggesting that each affected virus infection close to the same time. To further study this relationship and characterize the infection step affected by TPCs, we investigated viral colocalization with NPC1 or TPC2 (Fig. 3E). In untreated cells, VLPs were found in compartments containing both NPC1 and TPC2, as well as a distinct compartment containing only TPC2. However, treatment with tetrandrine significantly (and with other channel inhibitors less potently) increased accumulation of VLPs in the TPC2(+)/NPC1(+) compartment while proportionately decreasing TPC2(+)/NPC1(–) compartment colocalization (Fig. 3F). These results suggest that disrupting endosomal trafficking with tetrandrine potently alters viral distribution such that VLPs are retained in the NPC1(+) compartment.

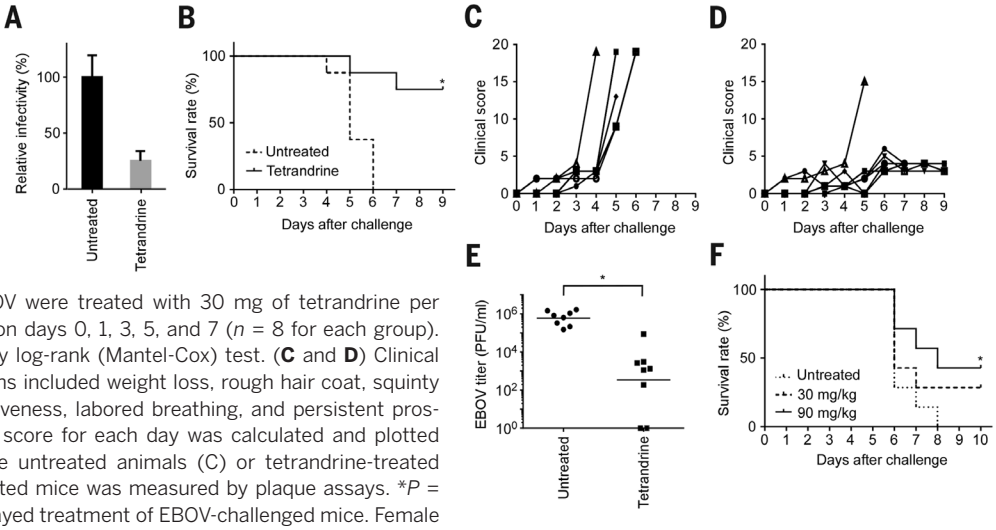

Fig. 4. Tetrandrine inhibits EBOV infection both in vitro and in vivo. (**A**) Macrophages were treated with tetrandrine (8 μM) and then infected with EBOV-GFP. After 48 hours, the frequency of GFP-positive cells was calculated and normalized to that of untreated controls. The data are the mean ± SD (n = 3) and representative of two independent experiments. (**B**) Female Balb/c mice injected intraperitoneally with mouse-adapted EBOV were treated with 30 mg of tetrandrine per kilogram of body weight or control saline on days 0, 1, 3, 5, and 7 (n = 8 for each group). Survival curves are shown. *P = 0.0008 by log-rank (Mantel-Cox) test. (**C** and **D**) Clinical scores of EBOV-infected mice. Disease signs included weight loss, rough hair coat, squinty eyes, hunched back, moderate unresponsiveness, labored breathing, and persistent prostration. Based on these criteria, a clinical score for each day was calculated and plotted (individually indicated by symbols) for the untreated animals (C) or tetrandrine-treated animals (D). (**E**) Virus titer in sera of infected mice was measured by plaque assays. *P = 0.006 by unpaired Student's t test. (**F**) Delayed treatment of EBOV-challenged mice. Female Balb/c mice injected intraperitoneally with mouse-adapted EBOV were treated with tetrandrine (30 or 90 mg/kg) or control saline on days 1, 3, 5, and 7 (n = 7 for each group). Survival curves are shown. *P = 0.04 by log-rank (Mantel-Cox) test comparing treated to untreated animals.

Because decreased colocalization with the TPC2 (+)/NPC1(−) compartment correlated with reduced infectivity, EBOV likely uses this compartment to enter host cells. Treatment with U18666A again resulted in VLP localization similar to that seen with calcium channel inhibitors (Fig. 3F). This may be explained by a recent report showing that U18666A treatment caused endosomal calcium depletion. Moreover, cells carrying a defective NPC1 were shown to have a loss of NAADP response, suggesting a close association of TPCs and NPC1 in host cells, which may affect EBOV infection (*26*).

Finally, we addressed whether TPC function could be targeted for anti-EBOV therapy. First, primary macrophages, an initial target of virus infection in humans and other animals, were evaluated. Similar to its effect in HeLa cells, tetrandrine potently blocked EBOV infection in human monocyte-derived macrophages, with verapamil and Ned19 being effective but requiring high doses (Fig. 4A and fig. S12) that did not show cytotoxicity. Of these, tetrandrine was the best candidate for animal testing because of its high potency and low cytotoxicity in culture. Moreover, the dose of tetrandrine needed to inhibit virus infection (IC_{50} = 55 nM) was at least a factor of 40 less than safe plasma concentrations achieved in mice and was reported to have good pharmacological properties, being well tolerated and having a long circulatory time (*27*). We therefore assessed therapeutic efficacy in the mouse model of EBOV disease (*28*). Mice were challenged with mouse-adapted EBOV and then given tetrandrine or saline every 2 days for 1 week. Starting tetrandrine treatment soon after infection significantly enhanced the survival of mice without any detectable side effects (Fig. 4B). Clinical scores in treated mice remained low compared to the control group (Fig. 4, C and D, and fig. S13). Virus titers in sera measured at day 3 after inoculation showed a factor of 1000 decrease (Fig. 4E), and by day 9 virus was undetectable. Furthermore, when the treatment was started 1 day after virus challenge, half the mice survived (Fig. 4F). These results indicate that tetrandrine is highly effective against disease in mice.

Taken together, we identified a role for TPCs in EBOV infection. These calcium channels appear responsible for controlling movement of endosomes containing virus particles. By disrupting TPC function, we prevented EBOV from escaping the endosomal network into the cell cytoplasm, halting infection. TPCs proved effective targets for existing drugs, with the bisbenzylisoquinoline alkaloid, tetrandrine, being the most potent. This may be due to its ability to block both TPC1 and TPC2, which regulate different stages of endosomal trafficking (*22*). Tetrandrine is one representative from this drug class; other members are found in plants around the world (*29*) and may also block EBOV infection. Because the entry of Marburgvirus, a distantly related filovirus, was also affected, it is likely that all filoviruses require TPC function to infect cells and that tetrandrine is a broad-spectrum filovirus inhibitor.

REFERENCES AND NOTES

1. H. Feldmann, T. W. Geisbert, *Lancet* **377**, 849–862 (2011).
2. S. Baize *et al.*, *N. Engl. J. Med.* **371**, 1418–1425 (2014).
3. B. M. Friedrich *et al.*, *Viruses* **4**, 1619–1650 (2012).
4. O. Dolnik, L. Kolesnikova, S. Becker, *Cell. Mol. Life Sci.* **65**, 756–776 (2008).
5. M. S. Boguski, K. D. Mandl, V. P. Sukhatme, *Science* **324**, 1394–1395 (2009).
6. C. P. Alvarez *et al.*, *J. Virol.* **76**, 6841–6844 (2002).
7. A. Takada *et al.*, *J. Virol.* **78**, 2943–2947 (2004).
8. A. S. Kondratowicz *et al.*, *Proc. Natl. Acad. Sci. U.S.A.* **108**, 8426–8431 (2011).
9. M. F. Saeed, A. A. Kolokoltsov, T. Albrecht, R. A. Davey, *PLOS Pathog.* **6**, e1001110 (2010).
10. A. Nanbo *et al.*, *PLOS Pathog.* **6**, e1001121 (2010).
11. K. Chandran, N. J. Sullivan, U. Felbor, S. P. Whelan, J. M. Cunningham, *Science* **308**, 1643–1645 (2005).
12. M. Côté *et al.*, *Nature* **477**, 344–348 (2011).
13. J. E. Carette *et al.*, *Nature* **477**, 340–343 (2011).
14. A. A. Kolokoltsov, M. F. Saeed, A. N. Freiberg, M. R. Holbrook, R. A. Davey, *Drug Dev. Res.* **70**, 255–265 (2009).
15. P. B. Madrid *et al.*, *PLOS ONE* **8**, e60579 (2013).
16. G. Gehring *et al.*, *J. Antimicrob. Chemother.* **69**, 2123–2131 (2014).
17. A. A. Genazzani *et al.*, *Br. J. Pharmacol.* **121**, 1489–1495 (1997).
18. A. Galione, *Cold Spring Harb. Perspect. Biol.* **3**, a004036 (2011).
19. E. Naylor *et al.*, *Nat. Chem. Biol.* **5**, 220–226 (2009).
20. M. Ruas *et al.*, *Curr. Biol.* **20**, 703–709 (2010).
21. P. J. Calcraft *et al.*, *Nature* **459**, 596–600 (2009).
22. M. X. Zhu *et al.*, *Am. J. Physiol. Cell Physiol.* **298**, C430–C441 (2010).
23. E. Brailoiu *et al.*, *J. Biol. Chem.* **285**, 38511–38516 (2010).
24. O. Martinez *et al.*, *Cell. Microbiol.* **12**, 148–157 (2010).
25. C. Grimm *et al.*, *Nat. Commun.* **5**, 4699 (2014).
26. E. Lloyd-Evans *et al.*, *Nat. Med.* **14**, 1247–1255 (2008).
27. C. L. Dai *et al.*, *Cancer Chemother. Pharmacol.* **60**, 741–750 (2007).
28. M. Bray, K. Davis, T. Geisbert, C. Schmaljohn, J. Huggins, *J. Infect. Dis.* **179** (suppl. 1), S248–S258 (1999).
29. C. Y. Kwan, F. I. Achike, *Acta Pharmacol. Sin.* **23**, 1057–1068 (2002).
30. R. Aarhus, R. M. Graeff, D. M. Dickey, T. F. Walseth, C. L. Hon, *J. Biol. Chem.* **270**, 30327–30333 (1995).
31. R. Parkesh *et al.*, *Cell Calcium* **43**, 531–538 (2008).
32. L. Arndt *et al.*, *Mol. Biol. Cell* **25**, 948–964 (2014).
33. X. Wang *et al.*, *Cell* **151**, 372–383 (2012).
34. C. Cang *et al.*, *Cell* **152**, 778–790 (2013).
35. C. Cang, B. Bekele, D. Ren, *Nat. Chem. Biol.* **10**, 463–469 (2014).

ACKNOWLEDGMENTS

All BSL4 work was performed at Texas Biomedical Research Institute by Y.S. and veterinary staff. For advice about preparation of NAADP-AM, we thank G. Churchill. For guidance and use of their high-performance liquid chromatography system, we thank A. Hayhurst and L. Sherwood. We thank D. Ren (University of Pennsylvania) for guidance in using the modified patch clamp. A. Reyes and J. Bentz provided technical support. O. Shtanko and M. Anantpadma gave helpful discussions and advice. We also thank all those cited in Materials and Methods for reagents. The data presented in this manuscript are tabulated in the main paper and in the supplementary materials. R.A.D and A.A.K. are inventors on U.S. patent 8,889,743, issued 28 November 2014, entitled "Inhibition of filovirus entry into cells and uses thereof." This work was supported by NIH R01AI063513, DOD/DTRA HDTRA1-12-1-0002, Project FRBAA09-6H-2-0043, the Ewing Halsell Foundation, and SFB TRR 152 TP04, TP05, TP06, and TP12.

SUPPLEMENTARY MATERIALS

www.sciencemag.org/content/347/6225/995/suppl/DC1
Materials and methods
Figs. S1 to S13

15 July 2014; accepted 20 January 2015
10.1126/science.1258758

ARCHAEOLOGY

Sedimentary DNA from a submerged site reveals wheat in the British Isles 8000 years ago

Oliver Smith,[1] Garry Momber,[2] Richard Bates,[3] Paul Garwood,[4] Simon Fitch,[5] Mark Pallen,[6]* Vincent Gaffney,[7]* Robin G. Allaby[1]*†

The Mesolithic-to-Neolithic transition marked the time when a hunter-gatherer economy gave way to agriculture, coinciding with rising sea levels. Bouldnor Cliff, is a submarine archaeological site off the Isle of Wight in the United Kingdom that has a well-preserved Mesolithic paleosol dated to 8000 years before the present. We analyzed a core obtained from sealed sediments, combining evidence from microgeomorphology and microfossils with sedimentary ancient DNA (sedaDNA) analyses to reconstruct floral and faunal changes during the occupation of this site, before it was submerged. In agreement with palynological analyses, the sedaDNA sequences suggest a mixed habitat of oak forest and herbaceous plants. However, they also provide evidence of wheat 2000 years earlier than mainland Britain and 400 years earlier than proximate European sites. These results suggest that sophisticated social networks linked the Neolithic front in southern Europe to the Mesolithic peoples of northern Europe.

The Mesolithic-to-Neolithic transition is associated with the replacement of a hunter-gatherer economy by arable farming of crops such as einkorn, emmer, and barley. Although it is generally accepted that the Neolithic had arrived by 6000 years before the present (yr B.P.) on the British mainland, controversy surrounds the timing and mode of Neolithization in the British Isles (*1*). It also remains unclear whether the arrival of Neolithic technologies on the mainland was rapid, facilitated by the arrival of migrating farmers, who displaced or acculturated existing hunter-gatherers (*2*); or whether hunter-gatherers gradually transitioned to

Two-pore channels control Ebola virus host cell entry and are drug targets for disease treatment

Yasuteru Sakurai *et al.*

Science **347**, 995 (2015);
DOI: 10.1126/science.1258758